# Mapping molecular orientation and conformation at interfaces by surface nonlinear optics

X. Zhuang,* P. B. Miranda, D. Kim,† and Y. R. Shen‡
*Department of Physics, University of California, Berkeley, California 94720-7300*
*and Materials Sciences Division, Lawrence Berkeley National Laboratory, Berkeley, California 94720*
(Received 6 November 1998)

Second-order nonlinear optics can be used to quantitatively determine the orientation of chemical bonds or submoieties of a fairly complicated molecule at an interface, and therefore completely map out its orientation and conformation. As a specific example, we have studied pentyl-cyanoterphenyl molecules at the air-water interface. We have measured the orientation of all three parts of the molecule (cyano head group, terphenyl ring, and pentyl chain) by optical second-harmonic generation and infrared-visible sum-frequency generation. A quantitatively consistent picture of the molecular configuration has been obtained. The technique can be applied to situations where other methods would fail (e.g., the surface of neat liquids or buried interfaces). [S0163-1829(99)04119-3]

## I. INTRODUCTION

Our ability of surface characterization directly affects the progress of surface science, a field of great importance to many disciplines ranging from physics and chemistry to life science and modern electronic technology. Among the various surface properties, molecular orientation is of special interest for its relevance to a wide variety of interesting phenomena such as adhesion, lubrication, catalysis, and biomembrane functions.[1] Many experimental techniques exist for surface studies,[2,3] but only a few can give quantitative information about molecular orientation at an interface. Each has its own shortcomings. Electron scattering[4] and electron-energy-loss spectroscopy,[5] or any other techniques involving particle scattering can only be operated with samples in high vacuum. Neutron scattering[6,7] and x-ray diffraction[7] require large experimental facilities or the studied surface must be to certain extent crystalline. The latter is also true for optical techniques like Brewster angle microscopy[8,9] and Brewster angle autocorrelation spectroscopy.[10] Other optical techniques, such as infrared[11,12] (IR), Raman,[13,14] or ultraviolet visible[15] spectroscopy and ellipsometry,[16] can be applied to any interfaces accessible by light, but they usually lack sufficient surface specificity to discriminate against bulk contributions.

Recently, second-harmonic generation (SHG) and sum-frequency generation (SFG) have been developed into very useful surface analytical probes.[17–22] They possess all the common advantages of optical techniques, namely, nondestructive, highly sensitive with good spatial, temporal, and spectral resolution, and applicable to any interfaces accessible by light. Being second-order nonlinear optical processes, they are forbidden in media with inversion symmetry, but allowed at interfaces where the inversion symmetry is necessarily broken. Consequently, they are intrinsically surface specific for interfaces between centrosymmetric media. If the input or output frequency is tuned over resonances the output is expected to be resonantly enhanced. Thus, SHG and SFG can also serve as surface spectroscopic tools. While SHG has been used to probe electronic transitions,[17,18,21] IR-visible SFG allows studies of surface vibrational resonances.[20–24] In both cases, the process is governed by a rank-three second-order nonlinear susceptibility tensor that characterizes the nonlinear response of the surface. Determination of the nonvanishing susceptibility elements from SHG or SFG can provide information on the average orientation of the molecules or selected sections of the molecules at an interface.[25–33] SHG probes electronic response of the surface molecules and is often less selective. Near a resonance, however, it could still be dominated by contribution from a selected part of the molecules. IR-visible SFG probes vibrational resonances that are generally associated with specific moieties or functional groups on the molecules. Thus, in principle, these techniques allow us to selectively study different parts of the molecules, particularly their orientations, and completely map out the orientation and conformation of the molecules at the surface or interface. In this paper, we would like to show that this is indeed the case.

We choose 4″-*n*-pentyl-4-cyano-*p*-terphenyl [5CT, $CH_3(CH_2)_4(C_6H_4)_3CN$) molecules at the air-water interface as a demonstrating system in our experiment. The 5CT molecules are amphiphilic and can form a Langmuir monolayer on water surface. Characterizing the molecular orientation and structure of Langmuir monolayers is of great importance, as they are often used as model systems for studying the function and structure of biomembranes,[34] which are mainly composed of one or two of such monolayers. For our purpose, a 5CT molecule can be divided into three sections: a cyano head group, a terphenyl ring, and an alkyl chain (see Fig. 1). We can separately measure the orientations of the

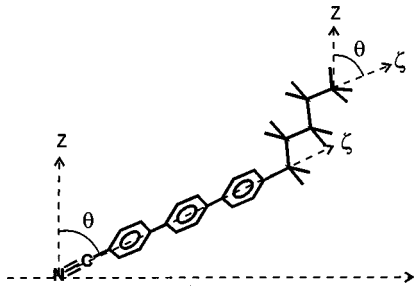


FIG. 1. Chemical structure of 5CT.

 

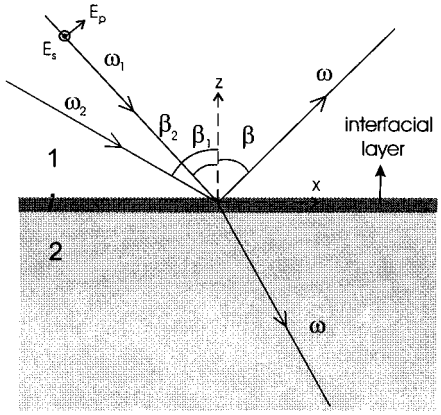


FIG. 2. Geometry for SHG and SFG from an interface in the reflection direction.

cyano group and alkyl chain by IR-visible SFG and that of the terphenyl ring by SHG. From the results, we can deduce the conformation and overall orientation of the molecules. As a check, we can compare the deduced 5CT conformation with the accepted one. However, as shown in Sec. II, the analysis to deduce the orientation of a moiety from SHG or SFG relies on the knowledge of the effective refractive index $n'$ for the interfacial layer. In previous studies, $n'$ was usually chosen to be equal to the refractive index of one of the two neighboring media,[25,35–37] and the deduced orientation would depend on the value of $n'$. In some studies, $n'$ was taken as the bulk refractive index of the monolayer material,[36,38] and in others, it was estimated from certain measurements[27,29,39–41] (ellipsometry, Kramers-Kronig analysis, etc). In this paper, we show that in order for our results to be physically reasonable and the deduced 5CT molecular conformation to be consistent with the commonly accepted one, we must have a value of $n'$ different from the bulk refractive index of 5CT and intermediate between those of the neighboring media, namely, air and water. With $n' = 1.18 \pm 0.04$, we find that the 5CT molecules adsorbed at the air/water interface with a tilt angle of $51.5° \pm 1.5°$ from the surface normal. This experimentally determined value for $n'$ is justified with a simple model calculation.

The paper is organized as follows. In Sec. II, we describe the basic theory of surface SHG and SFG measurements that can yield information on molecular orientations. Section III sketches the experimental system and the sample preparation method. The experimental results are presented in Sec. IV, describing how results are obtained and analyzed for the three sections of the 5CT molecule separately: alkyl chain, cyano group, and terphenyl ring. Then a brief discussion section concludes the article.

## II. THEORY

The basic theory of SHG and SFG as general surface analytical probes has been described elsewhere[17–22] and will not be repeated here. However, for the work to be reported in this paper, we need a careful description of how we can derive molecular orientation information from SHG and SFG. We generally treat an interfacial system as a three-layer system (Fig. 2) composed of two centrosymmetric media 1 and 2 and an interfacial layer. The interfacial layer can be either a bare interface or an interface with a layer of adsorbates. In the special case we shall discuss later, medium 1 is air and medium 2 water, and the interface has a 5CT monolayer adsorbed on water. Under the irradiation of two optical fields $\mathbf{E}_1$ and $\mathbf{E}_2$ with frequencies $\omega_1$ and $\omega_2$, respectively, a second-order nonlinear polarization $\mathbf{P}^{(2)}(\omega=\omega_1+\omega_2)$ is generated in the interfacial layer

$$\mathbf{P}^{(2)}(\omega=\omega_1+\omega_2)=\chi^{(2)}_{\mathrm{eff}}(\omega=\omega_1+\omega_2):\mathbf{E}_1(\omega_1)\mathbf{E}_2(\omega_2), \tag{1}$$

where $\chi^{(2)}_{\mathrm{eff}}(\omega=\omega_1+\omega_2)$ is the effective second-order nonlinear susceptibility tensor of the interface. For IR-visible SFG, $\omega_1$ is in the visible range and $\omega_2$ in the IR range. For SHG, $\omega_1=\omega_2$ and $\mathbf{E}_1=\mathbf{E}_2$. Under the electric-dipole approximation, the nonlinear polarization generated in media 1 and 2 must vanish due to inversion symmetry. The interfacial polarization sheet is then often the dominating source of radiation for SFG and SHG in the reflected direction. The sum-frequency intensity in the reflected direction is given by

$$I(\omega)=\frac{8\pi^3\omega^2\sec^2\beta}{c^3 n_1(\omega)n_1(\omega_1)n_1(\omega_2)}|\chi^{(2)}_{\mathrm{eff}}|^2 I_1(\omega_1)I_2(\omega_2), \tag{2}$$

where $n_i(\Omega)$ is the refractive index of medium $i$ at frequency $\Omega$, $\beta$ is the reflection angle of the sum-frequency field, $I_1(\omega_1)$ and $I_2(\omega_2)$ are the intensities of the two input fields. The effective nonlinear susceptibility $\chi^{(2)}_{\mathrm{eff}}$ takes the form of

$$\chi^{(2)}_{\mathrm{eff}}=[\hat{\mathbf{e}}(\omega)\cdot\mathbf{L}(\omega)]\cdot\chi^{(2)}:[\mathbf{L}(\omega_1)\cdot\hat{\mathbf{e}}(\omega_1)][\mathbf{L}(\omega_2)\cdot\hat{\mathbf{e}}(\omega_2)] \tag{3}$$

with $\hat{\mathbf{e}}(\Omega)$ being the unit polarization vector and $\mathbf{L}(\Omega)$ the Fresnel factor at frequency $\Omega$.

In the case of an azimuthally isotropic interface, there are only four independent nonvanishing components of $\chi^{(2)}$. With the lab coordinates chosen such that $z$ is along the interface normal and $x$ in the incidence plane, they are $\chi_{xxz}=\chi_{yyz}$, $\chi_{xzx}=\chi_{yzy}$, $\chi_{zxx}=\chi_{zyy}$, and $\chi_{zzz}$. These four components can be deduced by measuring SFG with four different input and output polarization combinations, namely, SSP (referring to *S*-polarized sum-frequency field, *S*-polarized $\mathbf{E}_1$, and *P*-polarized $\mathbf{E}_2$, respectively), SPS, PSS, and PPP. The effective nonlinear susceptibilities under these four polarization combinations can be expressed as

$$\chi^{(2)}_{\mathrm{eff,SSP}}=L_{yy}(\omega)L_{yy}(\omega_1)L_{zz}(\omega_2)\sin\beta_2\chi_{yyz}, \tag{4a}$$

$$\chi^{(2)}_{\mathrm{eff,SPS}}=L_{yy}(\omega)L_{zz}(\omega_1)L_{yy}(\omega_2)\sin\beta_1\chi_{yzy}, \tag{4b}$$

$$\chi^{(2)}_{\mathrm{eff,PSS}}=L_{zz}(\omega)L_{yy}(\omega_1)L_{yy}(\omega_2)\sin\beta\chi_{zyy}, \tag{4c}$$

$$\begin{aligned}\chi^{(2)}_{\mathrm{eff,PPP}}=&-L_{xx}(\omega)L_{xx}(\omega_1)L_{zz}(\omega_2)\cos\beta\cos\beta_1\sin\beta_2\chi_{xxz}\\&-L_{xx}(\omega)L_{zz}(\omega_1)L_{xx}(\omega_2)\cos\beta\sin\beta_1\cos\beta_2\chi_{xzx}\\&+L_{zz}(\omega)L_{xx}(\omega_1)L_{xx}(\omega_2)\sin\beta\cos\beta_1\cos\beta_2\chi_{zxx}\\&+L_{zz}(\omega)L_{zz}(\omega_1)L_{zz}(\omega_2)\sin\beta\sin\beta_1\sin\beta_2\chi_{zzz},\end{aligned} \tag{4d}$$

where $\beta_i$'s are the incidence angles of the optical field $\mathbf{E}_i$, and $L_{xx}(\Omega)$, $L_{yy}(\Omega)$ and $L_{zz}(\Omega)$ are the diagonal elements of $\mathbf{L}(\Omega)$, given by

$$L_{xx}(\Omega)=\frac{2n_1(\Omega)\cos\gamma}{n_1(\Omega)\cos\gamma+n_2(\Omega)\cos\beta}, \tag{5a}$$

$$L_{yy}(\Omega)=\frac{2n_1(\Omega)\cos\beta}{n_1(\Omega)\cos\beta+n_2(\Omega)\cos\gamma}, \tag{5b}$$

$$L_{zz}(\Omega)=\frac{2n_2(\Omega)\cos\beta}{n_1(\Omega)\cos\gamma+n_2(\Omega)\cos\beta}\left(\frac{n_1(\Omega)}{n'(\Omega)}\right)^2. \tag{5c}$$

In the above equations, $n'(\Omega)$ is the refractive index of the interfacial layer, $\beta$ is the incidence angle of the beam in consideration, and $\gamma$ is the refracted angle $[n_1(\Omega)\sin\beta=n_2(\Omega)\sin\gamma]$. Since the interfacial layer is only one (or a few) monolayer thick, its refractive index can be different from that of its own bulk material and difficult to measure.[42] It is therefore the usual practice that $n'(\Omega)$ is chosen to be equal to either $n_1(\Omega)$, $n_2(\Omega)$, or the bulk refractive index of the material at the interface. However, as noticed previously[27,29,36] and shown later in this paper, the determination of molecular orientation is quite sensitive to the value of $n'(\Omega)$, and choosing $n'(\Omega)$ to be equal to $n_1(\Omega)$ or $n_2(\Omega)$ is not always a good approximation.

In the case of SHG, the last two subindices of $\chi_{ijk}$ are interchangeable.[43] Thus, there are only three nonvanishing independent $\chi$ components, $\chi_{xxz}=\chi_{yyz}=\chi_{xzx}=\chi_{yzy}$, $\chi_{zxx}=\chi_{zyy}$, and $\chi_{zzz}$. They can be deduced from measurement with three different input and output polarization combinations, PS, SM, and PP. Here, the first and second letters denote the output and input polarization, respectively, and M refers to the polarization midway between S and P. The effective nonlinear susceptibilities take the forms

$$\chi^{(2)}_{\mathrm{eff,PS}}=L_{zz}(\omega)[L_{yy}(\omega_1)]^2\sin\beta\chi_{zyy}, \tag{6a}$$

$$\chi^{(2)}_{\mathrm{eff,SM}}=L_{yy}(\omega)L_{zz}(\omega_1)L_{yy}(\omega_1)\sin\beta_1\chi_{yzy}, \tag{6b}$$

$$\begin{aligned}\chi^{(2)}_{\mathrm{eff,PP}}=&+L_{zz}(\omega)[L_{xx}(\omega_1)]^2\sin\beta\cos^2\beta_1\chi_{zxx}\\&-2L_{xx}(\omega)L_{zz}(\omega_1)L_{xx}(\omega_1)\cos\beta\sin\beta_1\cos\beta_1\chi_{xzx}\\&+L_{zz}(\omega)[L_{zz}(\omega_1)]^2\sin\beta\sin^2\beta_1\chi_{zzz}.\end{aligned} \tag{6c}$$

In the case where the interface is composed of molecules, $\chi^{(2)}$ is related to the molecular hyperpolarizability $\alpha^{(2)}$ by

$$\chi^{(2)}_{ijk}=N_s l_{ii}(\omega)l_{jj}(\omega_1)l_{kk}(\omega_2)\sum_{\xi,\eta,\zeta}\langle(\hat{\mathbf{i}}\cdot\hat{\xi})(\hat{\mathbf{j}}\cdot\hat{\eta})(\hat{\mathbf{k}}\cdot\hat{\zeta})\rangle\alpha^{(2)}_{\xi\eta\zeta}, \tag{7}$$

where $N_s$ is the surface density of molecules, $(\mathbf{i},\mathbf{j},\mathbf{k})$ and $(\xi,\eta,\zeta)$ are unit vectors along the lab and molecular coordinates, respectively, and $\boldsymbol{l}$ is a tensor describing the microscopic local-field correction and the angular brackets denote an average over the molecular orientational distribution. As discussed in the Appendix, in the determination of molecular orientation at an interface, the effect of $\boldsymbol{l}(\Omega)$ can be lumped into the refractive index $\boldsymbol{n}'(\Omega)$ in Eq. (5c). We can then omit $l_{ii}, l_{jj}, l_{kk}$ in Eq. (7) and write

$$\chi^{(2)}_{ijk}=N_s\sum_{\xi,\eta,\zeta}\langle(\hat{\mathbf{i}}\cdot\hat{\xi})(\hat{\mathbf{j}}\cdot\hat{\eta})(\hat{\mathbf{k}}\cdot\hat{\zeta})\rangle\alpha^{(2)}_{\xi\eta\zeta}. \tag{8}$$

In many cases of SHG and SFG, $\alpha^{(2)}$ can be associated with a well-defined section or moiety of the surface molecules. If $\alpha^{(2)}_{\xi\eta\zeta}$ is known, then the average orientation of the moiety can often be deduced from measurements of $\chi^{(2)}_{ijk}$ using Eq. (8). For example, this is the case for molecules possessing a rodlike charge-transfer chromophore. Surface SHG has become a commonly adopted technique to measure monolayer orientation of such molecules. With IR-visible SFG, if the IR frequency $(\omega_2)$ is near vibrational resonances, $\alpha^{(2)}$ and $\chi^{(2)}$ can be written as

$$\alpha^{(2)}=\alpha^{(2)}_{\mathrm{NR}}+\sum_q\frac{\alpha_q}{\omega_2-\omega_q+i\Gamma_d}, \tag{9}$$

$$\chi^{(2)}=\chi^{(2)}_{\mathrm{NR}}+\sum_q\frac{\chi_q}{\omega_2-\omega_q-i\Gamma_q}, \tag{10}$$

where the subscript NR refers to nonresonant contribution, $\alpha_q$ $(\chi_q)$, $\omega_q$, and $\Gamma_q$ denote the strength, resonant frequency, and damping constant of the $q$th vibrational mode, respectively. Each mode may be associated with a particular moiety on the molecule. Again, if $(\chi_q)_{ijk}$ can be obtained from the resonant feature in the SFG spectrum, and $(\alpha_q)_{\xi\eta\zeta}$ is known, then the average orientation of the selected moiety may be deduced.

Before ending this section, we will discuss a special case, relevant to our study. In this case, $\omega$ and $\omega_1$ are both far away from electronic resonances and the moiety is cylindrically symmetric with symmetry axis along $\zeta$, so that there are only two nonvanishing independent components in $\alpha^{(2)}$, $\alpha^{(2)}_{\xi\xi\zeta}=\alpha^{(2)}_{\eta\eta\zeta}$, and $\alpha^{(2)}_{\zeta\zeta\zeta}$. From Eq. (8), we find for an azimuthally isotropic surface

$$\chi_{xxz}=\chi_{yyz}=\tfrac{1}{2}N_s\alpha[\langle\cos\theta\rangle(1+r)-\langle\cos^3\theta\rangle(1-r)], \tag{11a}$$

$$\chi_{xzx}=\chi_{yzy}=\chi_{zxx}=\chi_{zyy}=\tfrac{1}{2}N_s\alpha(\langle\cos\theta\rangle-\langle\cos^3\theta\rangle)(1-r), \tag{11b}$$

$$\chi_{zzz}=N_s\alpha[r\langle\cos\theta\rangle+\langle\cos^3\theta\rangle(1-r)], \tag{11c}$$

where $\alpha=\alpha_{\zeta\zeta\zeta}$, $r=\alpha_{\xi\xi\zeta}/\alpha_{\zeta\zeta\zeta}$, and $\theta$ is the polar angle of the symmetry axis $\zeta$ with respect to the lab $z$ axis. Due to the high symmetry in the hyperpolarizability tensor, the number of nonvanishing independent $\chi$ components is reduced to three. They can be deduced from SFG measurement with three different input and output polarization combinations, for example, SSP, SPS, and PPP. Since an absolute determination of $N_s\alpha$ is not of interest here, we can determine more conveniently from the measurements the ratios of independent nonvanishing $\chi$ components. Then from Eq. (11), we can find the orientation $\theta$ and the depolarization ratio $\mathbf{r}$ of the moiety by assuming a $\delta$-function distribution for $\theta$.

## III. EXPERIMENTAL SECTION

In the IR-visible SFG experiment, an active-passive mode-locked Nd: yttrium aluminum garnet (YAG) laser at 1064 nm with 25 ps pulsewidth and 20 Hz repetition rate was

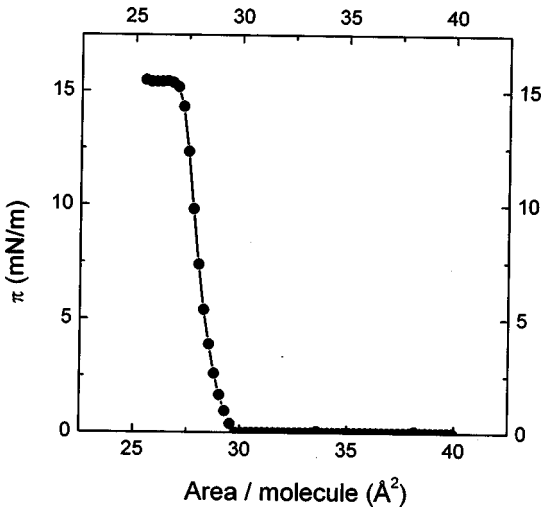


FIG. 3. Pressure-area isotherm for a 5CT monolayer on water.

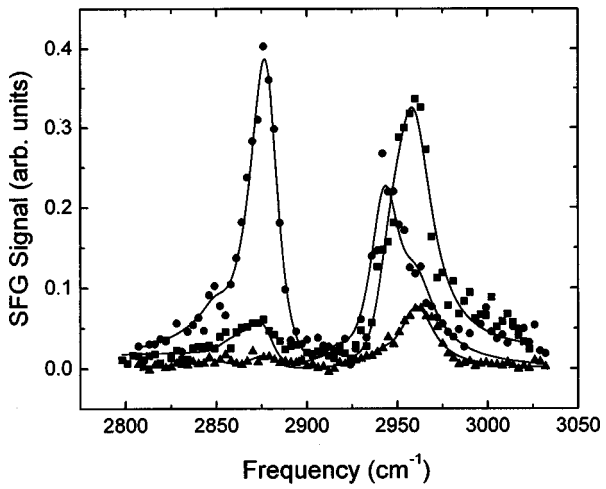


FIG. 4. SFG spectra for a 5CT monolayer on water in the CH stretch range. Circles, squares, and triangles are the experimental data obtained with SSP, PPP, and SPS polarizations, respectively. Solid lines are the fitting curves.

employed as the master light source. Its frequency-doubled output at 532 nm was used as the visible input. The tunable IR beam was generated in a $AgGaS_2$ crystal by difference-frequency mixing of the fundamental of the Nd:YAG laser with the output of an optical parametric generator/amplifier system pumped by the third harmonic of the laser.[44] The visible and IR beams were overlapped at the sample spatially and temporally with incidence angles 44° and 57°, respectively. The pulse energies and beam sizes were 1.5 mJ and 1.2 mm for the visible input and 70 to 110 $\mu$J and 0.6 mm for the infrared. The SF output in the reflected direction (reflected angle 45.5°) was detected by a photomultiplier with gated electronics after proper spatial and spectral filtering. In the SHG experiment, a frequency-doubled *Q*-switched mode-locked Nd:YAG laser at 532 nm and 500 Hz repetition rate was used as the fundamental beam. The second-harmonic output was again measured by a photomultiplier with gated electronics after a set of spectral filters. In both cases, the signal was attenuated when necessary to avoid saturation of the detection system.

The 5CT Langmuir monolayer was prepared by dissolving 5CT crystals (EM Industries) in chloroform (J. T. Baker, spectranalyzed grade) and spread on ultrapure water (resistivity of 18.3 MΩ·cm, Barnstead Easy-Pure) in a Teflon Langmuir trough. The film was then compressed slowly and the surface pressure was monitored by a Wilhelmy plate and a microbalance. The resulting pressure-area isotherm is shown in Fig. 3. All the SHG and SFG measurements were done on films with area per 5CT molecule around 28 Å$^2$. We also used in the experiment a full hexadecanol monolayer on water as a reference sample. It was prepared by placing a small crystal of hexadecanol on the surface of ultrapure water. The hexadecanol molecules spontaneously spread to form a stable full monolayer.[33]

## IV. RESULTS

The 5CT molecule is composed of a CN head group, a terphenyl-ring chromophore, and a $C_5$ alkyl chain. We discuss here the results of SFG and SHG measurements on the average orientation of each segment separately.

### A. Alkyl chain

We used SFG spectra of CH stretch modes to determine orientation and conformation of the alkyl chain of 5CT. Figure 4 shows the spectra of the 5CT Langmuir monolayer in this range, at three different input and output polarization combinations, SSP, SPS, and PPP. The solid curves in the figure were obtained by fitting using Eq. (10); the fitting parameters are listed in Table I. The peak assignments in the spectra of Fig. 4 are well known.[45] The vibrational modes at approximately 2875, 2960, and 2940 cm$^{-1}$ can be assigned, respectively, to the symmetric ($r^+$) and antisymmetric ($r^-$) stretches of the terminal $CH_3$ group of the alkyl chain and the Fermi resonance ($r_{FR}^+$) between the symmetric $CH_3$ stretch and its bending mode. The weak modes at ~2850 and ~2920 cm$^{-1}$ can be assigned to the symmetric ($d^+$) and antisymmetric ($d^-$) stretches of the $CH_2$ groups on the chain, respectively. The fact that the strengths of these modes are essentially negligible compared to those of $CH_3$ groups suggests that the alkyl chains are nearly all trans and contain few gauche defects.[46]

The orientation of the terminal $CH_3$ group can be determined by analyzing its symmetric stretch mode.[47] This mode has $C_{3v}$ symmetry and can only be excited if the IR polarization is along the symmetry axis. As a result, there are only two nonvanishing independent elements in the hyperpolariz-

TABLE I. Fitting parameters $\chi_q$, $\omega_q$, and $\Gamma_q$ of SFG spectra for 5CT monolayer on water.

| Mode | $\omega_q$ (cm$^{-1}$) | $\Gamma_q$ (cm$^{-1}$) | $\chi_{q,\mathrm{SSP}}$ | $\chi_{q,\mathrm{PPP}}$ | $\chi_{q,\mathrm{SPS}}$ |
|---|---|---|---|---|---|
| $d^+$ | 2852 | 8.0 | 0.43±0.23 | 0.21±0.36 | −0.42±0.41 |
| $r^+$ | 2878 | 8.7 | 5.18±0.52 | −1.52±0.18 | −0.97±0.31 |
| $d^-$ | 2917 | 10.0 | 0.67±0.34 | −0.80±0.36 | 0.02±0.76 |
| $r_{FR}^+$ | 2943 | 10.0 | 4.19±0.12 | −5.23±0.22 | −0.51±0.42 |
| $r^-$ | 2959 | 10.6 | 1.50±0.18 | 8.45±0.41 | −2.82±0.26 |
| CN stretch | 2233 | 7.3 | 13.55±1.30 | −3.17±0.43 | 5.35±0.50 |

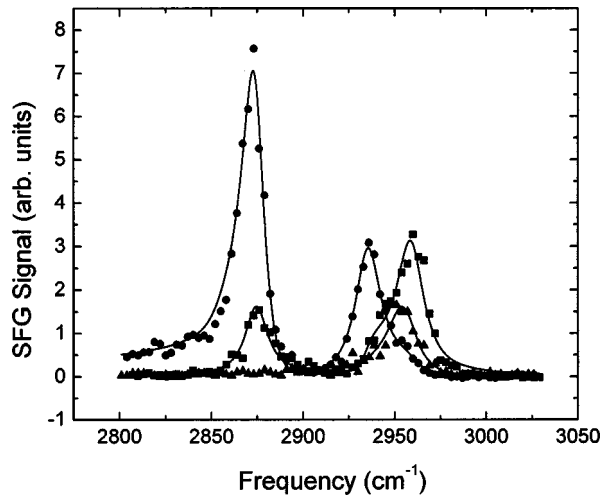


FIG. 5. SFG spectra for a hexadecanol monolayer on water in the CH stretch range. Circles, squares, and triangles are the experimental data obtained with SSP, PPP, and SPS polarizations, respectively. Solid lines are the fitting curves.

ability tensor, $\alpha_{\zeta\zeta\zeta}$ and $\alpha_{\xi\xi\zeta}=\alpha_{\eta\eta\zeta}=r\alpha_{\zeta\zeta\zeta}$. The polar angle $\theta$ and depolarization ratio $r$ can then be deduced from the $\chi_q$'s listed in Table I following Eqs. (4), (5), and (11). Using[48] $n_2(\mathrm{VIS})=1.337$, $n_2(\mathrm{IR})=1.393+0.013i$, $n_2(\mathrm{SF})=1.343$ and assuming $n'=n_1=1$ for all frequencies, we obtain $\theta=39°(+2°, -5°)$ and $r\geqslant 5.5$. This large value for $r$ is physically unreasonable. Although the value for $r$ is not agreed upon in the literature, it usually ranges from 1.66 to 3.5.[27,33] From the known bond geometry of the $CH_3$ group, one finds that $r$ cannot be larger than 4.2. The value deduced from Raman measurements and used in a previous SFG work is $2.3\pm 0.3$.[32]

We find that the same difficulty appears in the SFG results of hexadecanol monolayers on water as well. The IR-visible SFG spectra of a hexadecanol monolayer are shown in Fig. 5 with the fitting parameters given in Table II. Following the same procedure, we can again determine $\theta$ and $r$ for the terminal $CH_3$ groups of the hexadecanol monolayer. However, the $r^+$ mode in the SPS spectrum is nearly absent, so that we can only assess an upper value for $(\chi_{r+})_{\mathrm{SPS}}$, leading to a range of possible solutions: $0°<\theta<28°$ and $r>3.3$. A fully packed hexadecanol monolayer on water forms a two-dimensional crystalline structure and has been well studied by x-ray diffraction.[49] The hexadecanol chain has been found to be tilted 15.8° and 2.8° from the surface normal along the crystalline $b$ and $a$ axes of the monolayer, respectively. Furthermore, the two molecules in a unit cell have the planes of their hydrocarbon chains forming a dihedral angle of 120°. From this known herringbone arrangement of the molecules, we find that half of the $CH_3$ groups have a polar angle of 24.8° and the other half 20.6°. With this orientation for hexadecanol molecules, the values of $r$ that are consistent with the spectra in Fig. 5 are $6.6<r<14.9$, which again are physically unreasonable. We also notice in Figs. 4 and 5 that the $CH_3$ symmetric stretch peak is one order of magnitude stronger for hexadecanol than for 5CT. This would be difficult to understand if the above values of $\theta$ for hexadecanol and 5CT were correct, knowing that the areas per molecule for hexadecanol[49] and 5CT (20 Å$^2$ versus 28 Å$^2$) are comparable. All these difficulties seem to have originated from our assumption $n'=1$ in the analysis. In fact, Bain and coworkers also found a similar inconsistency in analyzing the SFG spectra for a dodecanol monolayer.[27] They concluded that in order to obtain the known upright orientation for dodecanol molecules, they must assume $n'\cong 1.2$ if $r$ is taken to be 3.5. It should be mentioned that taking a $\delta$ function for the orientational distribution of surface molecules is not the reason for the unphysical values of $r$ deduced from our data, with the assumption of $n'=1$. Introducing a tilt distribution does not bring the value of $r$ within the physically reasonable limits $(1.5<r<4)$ for values of $\chi$ components within our accuracy. In the following, we resolve this problem by simultaneously determining $n'$, $\theta_{5\mathrm{CT}}$ and $r$ using the hexadecanol monolayer as a reference.

TABLE II. Fitting parameters $\chi_q$, $\omega_q$, and $\Gamma_q$ of SFG spectra for a hexadecanol monolayer on water.

| Mode | $\omega_q$ (cm$^{-1}$) | $\Gamma_q$ (cm$^{-1}$) | $\chi_{q,\,\mathrm{SSP}}$ | $\chi_{q,\,\mathrm{PPP}}$ | $\chi_{q,\,\mathrm{SPS}}$ |
|---|---|---|---|---|---|
| $d^+$ | 2853 | 9.4 | $-1.2\ \pm 0.47$ | $-0.01\pm 1.00$ | $-0.50\pm 1.44$ |
| $r^+$ | 2875 | 6.8 | $17.63\pm 1.40$ | $-9.12\pm 0.90$ | $-0.08\pm 1.50$ |
| $d^-$ | 2919 | 10.0 | $-0.01\pm 0.54$ | $5.79\pm 3.69$ | $-0.10\pm 0.85$ |
| $r^+_{\mathrm{FR}}$ | 2936 | 7.8 | $14.35\pm 1.21$ | $-8.71\pm 1.78$ | $-0.72\pm 0.98$ |
| $r^-$ | 2959 | 9.0 | $-7.49\pm 2.75$ | $15.63\pm 1.20$ | $11.69\pm 1.63$ |

With the known orientation for hexadecanol molecules from the x-ray diffraction measurements, the number of parameters to be determined is reduced to three: $\theta_{5\mathrm{CT}}$, $r$, and $n'$. The SFG spectra in Figs. 4 and 5 give us five independent ratios of $\chi^{(2)}$ components for the $r^+$ mode, $\chi_{\mathrm{SPS}}/\chi_{\mathrm{SSP}}(5\mathrm{CT})$, $\chi_{\mathrm{PPP}}/\chi_{\mathrm{SSP}}(5\mathrm{CT})$, $\chi_{\mathrm{SPS}}/\chi_{\mathrm{SSP}}(C_{16}OH)$, $\chi_{\mathrm{PPP}}/\chi_{\mathrm{SSP}}(C_{16}OH)$, and $\chi_{\mathrm{SSP}}(5\mathrm{CT})/\chi_{\mathrm{SSP}}(C_{16}OH)$, from which the three parameters can be derived. However, the ratio $\chi_{\mathrm{SPS}}/\chi_{\mathrm{SSP}}(C_{16}OH)$ is very small and subject to a very large uncertainty, since the $r^+$ peak in the SPS spectrum of hexadecanol is practically absent. Also, the ratio $\chi_{\mathrm{SSP}}(5\mathrm{CT})/\chi_{\mathrm{SSP}}(C_{16}OH)$ depends on the ratio of surface densities of the two monolayers, which is an extra source of uncertainty. Therefore, we chose to use only the ratios $\chi_{\mathrm{SPS}}/\chi_{\mathrm{SSP}}(5\mathrm{CT})$, $\chi_{\mathrm{PPP}}/\chi_{\mathrm{SSP}}(5\mathrm{CT})$, and $\chi_{\mathrm{PPP}}/\chi_{\mathrm{SSP}}(C_{16}OH)$ in order to determine $\theta_{5\mathrm{CT}}$, $r$, and $n'$, with the other two used only for consistency check. Following Eqs. (4), (5), and (11), we can calculate these three ratios as a function of $\theta_{5\mathrm{CT}}$, $r$, and $n'$, assuming the known value of $\theta\cong 23°$ for hexadecanol deduced from the x-ray diffraction results.[49] The parameters $\theta_{5\mathrm{CT}}$, $r$, and $n'$ can then be determined by solving simultaneously the three equations. The results obtained are $\theta_{5\mathrm{CT}}=54°(+14°, -8°)$, $r=2.5(+1.7,-1.0)$, and $n'=1.18\pm 0.04$. The assumptions used in the above calculation are that $r$ and $n'$ for 5CT and hexadecanol are the same and the dispersion of $n'$ is negligible. That $r$ is the same in both cases is to be expected, considering that in both cases we are dealing with the terminal $CH_3$ group of an all-trans alkyl chain. Neglecting variations in $n'$ due to dispersion or the slightly different densities of the two monolayers is a simplifying assumption. However, the errors introduced by such an approximation are within the experimental uncertainty in determining $n'$. Note that the deduced value of $r$ agrees well with the Raman results. Using the values of $r$ and $n'$ deter-

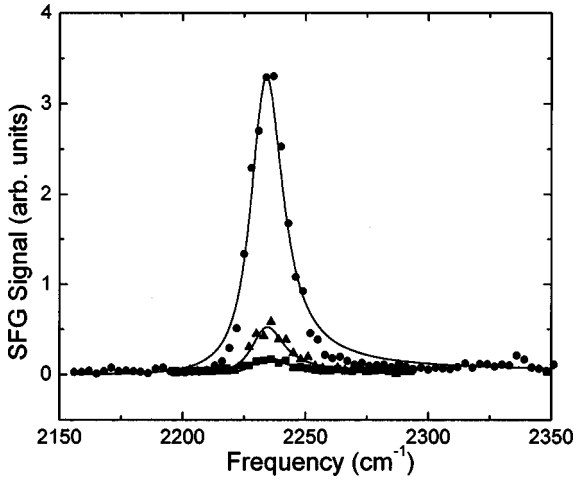


FIG. 6. SFG spectra for a 5CT monolayer on water in the CN stretch range. Circles, squares, and triangles are the experimental data obtained with SSP, PPP, and SPS polarizations, respectively. Solid lines are the fitting curves.

mined above and the tilt angles of the $CH_3$ groups of hexadecanol determined from the x-ray diffraction measurements, we can calculate from Eqs. (4), (5), and (11) the ratios $\chi_{SPS}/\chi_{SSP}=-0.037$ and $\chi_{PPP}/\chi_{SSP}=-0.52$ for the hexadecanol monolayer. They compare well with the measured ratios $-0.090<\chi_{SPS}/\chi_{SSP}<0$ and $\chi_{PPP}/\chi_{SSP}=-0.52\pm.09$ obtained from the values of SFG susceptibilities listed in Table II. This shows that our procedure is selfconsistent and supports the choice of $n'=1.18$ for both monolayers. This value of $n'$ is lower than bulk refractive indices of hexadecane[50] ($n=1.43$), hexadecanol[50] ($n=1.44$), and 5CT (Ref. 51) ($n_e=1.89$, $n_0=1.54$) but is not unreasonable since the $CH_3$ group is in contact with air and therefore has only a partial screening by nearby neighboring molecules. In the Appendix, we support this choice of $n'$ with a simple calculation based on a modified Lorentz model for local-field correction at the interface. In principle, the values for $n'$ for other moieties in the monolayer could be different, but in the following we will use the same $n'$ for all moieties and show that our results give a self-consistent picture of the molecular geometry at the interface.

### B. Cyano group

We used the CN stretch peak in SFG spectra to determine the orientation of the CN bond in 5CT. The spectra are shown in Fig. 6, where the single peak can be attributed to the stretching of the cyano triple bond. Fitting the spectra with Eq. (10) gives the resonant frequency, damping constant and strengths of this mode listed in the last row of Table I. The hyperpolarizability tensor of this mode again has only two nonvanishing independent components $\alpha_{\zeta\zeta\zeta}$ and $\alpha_{\xi\xi\zeta}=\alpha_{\eta\eta\zeta}=r\alpha_{\zeta\zeta\zeta}$ with $\zeta$ along the triple-bond direction. Using Eqs. (4), (5), and (11), we can deduce $\theta$ and $r$ for the CN bond from the measured ratios $\chi_{SPS}/\chi_{SSP}$ and $\chi_{PPP}/\chi_{SSP}$. Taking[48] $n_2(\mathrm{VIS})=1.337$, $n_2(\mathrm{IR})=1.315+0.011i$, $n_2(\mathrm{SF})=1.342$, and using $n'=1.18\pm0.04$ as determined above from the CH spectra, we find that $\theta=53°\pm3°$ and $r=0.25\pm0.03$. In this case, we have no *a priori* reason to choose $n'=1.18$. Considering that the CN groups are buried under the monolayer, in contact with water, we would expect $n'$ to be somewhat larger than 1.18, possibly close to the value of bulk water ($n=1.34$). This would lead to smaller $\theta$ and $r$. We shall come back to this point in the discussion section.

### C. Terphenyl chromophore

We determined the orientation of the terphenyl chromophore by SHG. This has been studied before with a less complete measurement and analysis.[35] As is well understood, the SHG from 5CT comes mainly from the terphenyl part where the electron cloud is highly delocalized, yielding a large optical nonlinearity. Therefore, SHG can be used to selectively measure the orientation of the chromophore. As discussed in the Sec. II, only three nonvanishing independent $\chi$ components exist for an azimuthally isotropic surface, which can be determined by measuring SHG with polarization combinations PS, SM, and PP. To extract information on the chromophore orientation from these $\chi$ components, once again we need to have some knowledge about the hyperpolarizability tensor. In this case, the second harmonic frequency is in resonance with an electronic transition of 5CT involving an excited state that has an electron redistribution along the long axis of the terphenyl ring $\zeta$.[35] Therefore, the $\alpha^{(2)}$ components whose first index is $\zeta$ should be dominant. We will also assume that the terphenyl ring is cylindrically symmetric about the $\zeta$ axis. This assumption is motivated by the fact that the phenyl rings in the chromophore do not lie all in the same plane: paraterphenyl molecules have twist angles between adjacent phenyl rings ranging from 15° to 27° in a low-temperature phase.[52] 5CB molecules (similar to 5CT, but with only two phenyl rings) have a twist angle of 26° in the crystalline phase[53] and 38° in the nematic phase.[54] With these assumptions, the hyperpolarizability tensor contains two significant nonvanishing independent elements $\alpha_{\zeta\zeta\zeta}$ and $\alpha_{\zeta\xi\xi}=\alpha_{\zeta\eta\eta}=r\alpha_{\zeta\zeta\zeta}$. From the experimentally determined ratios $\chi_{SM}/\chi_{PS}=1.16\pm0.04$ and $\chi_{PP}/\chi_{PS}=0.55\pm0.05$, we deduce $\theta=50.0°\pm2.5°$ and $r=-0.050\pm0.006$ for the terphenyl chromophore using Eqs. (5), (6), and (11) [with the first and last subindices of $\chi_{ijk}$ exchanged in Eq. (11)] and[48] $n_2(\mathrm{VIS})=1.337$, $n_2(\mathrm{SH})=1.381$, and $n'=1.18\pm0.04$. Again, we have no *a priori* reason to choose $n'=1.18$ here. A larger $n'$ could yield a smaller $\theta$. We also note that the above determined value of $r=-0.050$ is quite small, implying that our assumption about the axial symmetry of the terphenyl core does not have a significant effect on the value of $\theta$.

## V. DISCUSSION

The chemical structure of 5CT molecule is shown in Fig. 1. According to this picture, the polar angles of the cyano group and terphenyl chromophore should be equal to each other. If the alkyl chain takes an all-trans conformation, as suggested by the weakness of the $d^+$ mode in the SFG spectrum of Fig. 4, the polar angle of the terminal $CH_3$ group should also take the same value. The polar orientation deduced from our SHG and SFG measurement agrees well with this picture. The measured polar angles of the cyano group ($53°\pm3°$), terphenyl ring ($50.0°\pm2.5°$) and terminal $CH_3$

group [54°(+14°, −8°)] all agree within the experimental uncertainty. Combining the above measurements we can conclude that the 5CT polar angle is $51.5° \pm 1.5°$. However, this orientation is quite different from the value obtained previously[35] for the chromophore (60°) from SHG measurements by assuming $n' = 1$, indicating again the importance of its proper determination. In this earlier measurement, the assumption of $n' = 1$ was supported by the linear relationship between the square root of SHG signal and monolayer density. This can only be true if $n'$ does not depend on density, which is only true for $n' = 1$. However, from the scatter in the data and limited monolayer density range studied, a small change in linearity caused by $n' \approx 1.2$ at full coverage could not be easily detected.

We should now comment on the values of $n'$ used in the data analysis. As shown by the simple calculation in the Appendix, the value $n' = 1.18$ determined from SFG measurements for the terminal $CH_3$ group is not unreasonable, considering that this group is right at the interface between air and the rest of the monolayer and therefore has only a partial screening by neighboring molecules. However, the use of $n' = 1.18$ for the analysis of terphenyl chromophore and CN orientations is less justifiable. Intuitively, one would expect that $n'$ for the terphenyl chromophore and CN would assume values very close to the bulk refractive indices of the monolayer material and the water subphase, respectively. The polar angles obtained would be 30° for the terphenyl chromophore (taking $n' = 1.60$) and 41° for the CN group (taking $n' = 1.34$). These values are in clear disagreement with the $CH_3$ orientation, even with its large error bar. Therefore, the value of $n'$ for the core part cannot be considerably larger than the value 1.18 determined for the $CH_3$ group. This suggests that the proper value for $n'$ for the analysis of SFG or SHG measurements has to be determined with care. It may not necessarily be the same as the bulk refractive index of the material at the interface or the one determined by ellipsometry ($n_e' = 1.49$, $n_0' = 1.46$ for a dodecanol monolayer at the air/water interface[42]), since the effective $n'$ depends on the local-field correction and on which moiety being probed. In this paper, we have used a hexadecanol monolayer as a reference system of known orientation to determine $n'$. The same value of $n'$ can then be used for other monolayers with $CH_3$-terminated alkyl chains, as long as their surface densities are close to that of the hexadecanol monolayer.

To conclude, we have shown that the second-order nonlinear optical processes, SFG and SHG, can be used to quantitatively determine the average orientation of selective functional groups or moieties of surface molecules. The combined results allow us to completely map out the orientation and conformation of a fairly complicated molecule at an interface. The 5CT Langmuir monolayer is chosen as a demonstrating system. The orientations of all three parts of the molecule, cyano group, terphenyl ring, and pentyl chain, have been measured separately by optical SHG and SFG. The results give a quantitatively consistent picture of the molecular configuration if the appropriate refractive indices for the monolayer are used. The latter can be obtained from measurements on a similar monolayer of known orientation.

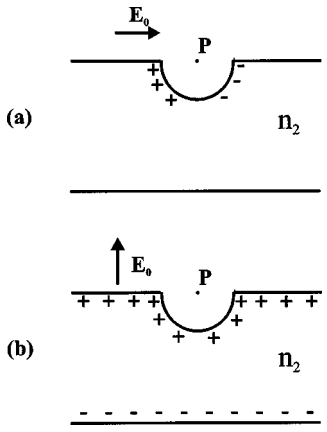


FIG. 7. Slab model for calculation of local-field correction at the interface. The incident field $E_0$ is (a) parallel and (b) perpendicular to the interface.


## ACKNOWLEDGMENTS

We would like to acknowledge useful discussions with Xing Wei. This work was supported by the Lawrence Berkeley Laboratory through the Director, Office of Energy Research, Basic Energy Science, Materials Science Division of the U.S. Department of Energy under Contract No. DE-AC03-76SF00098.


## APPENDIX

Here we hope to justify the value of $n' = 1.18$ determined for the hexadecanol and 5CT monolayers with a simple estimate of the local-field correction at the interface using a modified Lorentz model.[55] In calculating the orientation of a moiety, we need to know the ratio of $\chi^{(2)}$ elements, for example, $\chi^{(2)}_{\text{eff, SPS}}/\chi^{(2)}_{\text{eff, SSP}}$. We consider the moiety at the interface between media 1 and 2 with refractive indices $n_1$ and $n_2$, respectively. From Eqs. (4) and (7), we can write

$$\frac{\chi^{(2)}_{\text{eff,SPS}}}{\chi^{(2)}_{\text{eff,SSP}}} = \frac{\sin\beta_1}{\sin\beta_2}\left(\frac{L_{zz}l_{zz}}{L_{yy}l_{yy}}\right)_{\omega_1}\left(\frac{L_{yy}l_{yy}}{L_{zz}l_{zz}}\right)_{\omega_2}\frac{\langle\alpha^{(2)}_{yzy}\rangle}{\langle\alpha^{(2)}_{yyz}\rangle}, \quad \text{(A1)}$$

where $\langle\alpha^{(2)}_{ijk}\rangle = \Sigma_{\xi,\eta,\zeta}\langle(\hat{\mathbf{i}}\cdot\hat{\xi})(\hat{\mathbf{j}}\cdot\hat{\eta})(\hat{\mathbf{k}}\cdot\hat{\zeta})\rangle\alpha^{(2)}_{\xi\eta\zeta}$ and $L_{ii}(\Omega)$ is given in Eq. (5) except that in $L_{zz}(\Omega)$, $n'$ is taken as $n_1$. From the three-layer model (Fig. 2), however, we find

$$\frac{\chi^{(2)}_{\text{eff,SPS}}}{\chi^{(2)}_{\text{eff,SSP}}} = \frac{\sin\beta_1}{\sin\beta_2}\left(\frac{L_{zz}(n')}{L_{yy}}\right)_{\omega_1}\left(\frac{L_{yy}}{L_{zz}(n')}\right)_{\omega_2}\frac{\langle\alpha^{(2)}_{yzy}\rangle}{\langle\alpha^{(2)}_{yyz}\rangle} \quad \text{(A2)}$$

with $L_{ii}(\Omega)$ given in Eq. (5). Comparison of Eqs. (A.1) and (A.2) then yields, at each $\omega$,

$$\frac{l_{zz}}{l_{yy}} = \left(\frac{n_1}{n'}\right)^2. \quad \text{(A3)}$$

This result can be proved to be true in general. To find $n'$, we must evaluate $l_{zz}$ and $l_{yy}$. Consider the geometry shown in Fig. 7, where we have assumed $n_1 = 1$ for simplicity. The extension to the case of $n_1 \neq 1$ is straightforward. We want to

calculate the local field at the point $P$ at the surface for the input field parallel [Fig. 7(a)] or perpendicular [Fig. 7(b)] to the surface. The local field at $P$ is the sum of the input field and the dipole fields generated by polarizations inside the hemisphere around $P$ and in the rest of the semi-infinite medium. Because of the assumed isotropic symmetry of the medium, dipole field from the polarization in the hemisphere vanishes and $E_P$ is given by

$$E_P = E_0 + E_{\text{surf}}, \tag{A4}$$

where $E_{\text{surf}}$ is the contribution from the bound charges at the slab surface, as shown in Fig. 7. We can calculate $E_{\text{surf}}$ in the electrostatic limit. The results for $E_0$ parallel and perpendicular to the surface are

$$E_P^{\parallel} = E_0^{\parallel} - \frac{n_2^2-1}{3n_2^2} E_0^{\parallel} = E_0^{\parallel}\left(\frac{2n_2^2+1}{3n_2^2}\right), \quad \text{with } E_0^{\parallel} \| z \tag{A5}$$

$$E_P^{\perp} = E_0^{\perp} + \frac{n_2^2-1}{6} E_0^{\perp} = E_0^{\perp}\left(\frac{n_2^2+5}{6}\right), \quad \text{with } E_0^{\perp} \perp z. \tag{A6}$$

Knowing $l_{xx} = l_{yy} = E_P^{\perp}/E_0^{\perp}$ and $l_{zz} = E_P^{\parallel}/E_0^{\parallel}$, we then get from Eq. (A.3)

$$\left(\frac{1}{n'}\right)^2 = \frac{(2n_2^2+1)/(3n_2^2)}{(n_2^2+5)/6} = \frac{4n_2^2+2}{n_2^2(n_2^2+5)}. \tag{A7}$$

The above equation gives $n' = 1.22$ for $n_2 = 1.5$ (close to the value for hydrocarbons) and $n' = 1.15$ for $n_2 = 1.34$ (close to the value for water). The value of $n' = 1.18$ we used in the data analysis is between these two values. This means that for any reasonable choice for $n_2$ the value of $n'$ calculated from this simple model is close to 1.18, which, as we have shown in this paper, does give a consistent picture of the 5CT orientation and conformation within our experimental uncertainty.

*Present address: Department of Physics, Stanford University, Stanford, CA 94305.

†Present address: Department of Physics, Sogang University, Seoul, 100-611, Korea.

‡Author to whom correspondence should be addressed. Electronic address: shenyr@socrates.berkeley.edu

[1] A. W. Adamson and A. P. Gast, *Physical Chemistry of Surfaces* 6th ed. (Wiley-Interscience, New York, 1997).

[2] A. Zangwill, *Physics at Surfaces* (Cambridge University Press, Cambridge, 1988).

[3] See, for example, *Surface Science: The First Thirty Years,''* edited by C. B. Duke, special issue of Surf. Sci. **299/300** (1994).

[4] R. E. Palmer and P. J. Rous, Rev. Mod. Phys. **64**, 383 (1992).

[5] P. Avouris and J. Demuth, Annu. Rev. Phys. Chem. **35**, 49 (1984).

[6] J. R. Lu, Z. X. Li, J. Smallwood, R. K. Thomas, and J. Penfold, J. Phys. Chem. **99**, 8233 (1995).

[7] J. Als-Nielsen, D. Jacquemain, K. Kjaer, F. Leveiller, M. Lahav, and L. Leiserowitz, Phys. Rep. **246**, 251 (1994).

[8] K. Hosoi, T. Ishikawa, A. Tomioka, and K. Miyano, Jpn. J. Appl. Phys., Part 2 **32**, L135 (1993).

[9] M. W. Tsao, T. M. Fischer, and C. M. Knobler, Langmuir **11**, 3184 (1995).

[10] C. Lautz, Th. M. Fischer, M. Weygland, M. Lösche, P. B. Howes, and K. Kjaer, J. Chem. Phys. **108**, 4640 (1998).

[11] R. Mendelsohn, J. W. Brauner, and A. Gericke, Annu. Rev. Phys. Chem. **46**, 305 (1995).

[12] D. J. Neivandt, M. L. Gee, M. L. Hair, and C. P. Tripp, J. Phys. Chem. B **102**, 5107 (1998).

[13] M. A. Hines, T. D. Harris, A. L. Harris, and Y. J. Chabal, J. Electron Spectrosc. Relat. Phenom. **64/65**, 183 (1993).

[14] T. Sueoka, J. Inukai, and M. Ito, J. Electron Spectrosc. Relat. Phenom. **64/65**, 363 (1993).

[15] M. D. Elking, G. He, and Z. Xu, J. Chem. Phys. **105**, 6565 (1996).

[16] I. Hirosawa, Jpn. J. Appl. Phys., Part 1 **36**, 5192 (1997).

[17] Y. R. Shen, Annu. Rev. Phys. Chem. **40**, 327 (1989).

[18] G. L. Richmond, J. M. Robinson, and V. L. Shannon, Prog. Surf. Sci. **28**, 1 (1988).

[19] T. F. Heinz, in *Nonlinear Surface Electromagnetic Phenomena*, edited by H. E. Ponath and G. I. Stegeman (North-Holland, Amsterdam, 1991), pp. 353–416.

[20] Y. R. Shen, Surf. Sci. **299/300**, 551 (1994).

[21] K. B. Eisenthal, Chem. Rev. **96**, 1343 (1996).

[22] C. D. Bain, J. Chem. Soc., Faraday Trans. **91**, 1281 (1995).

[23] A. Tadjeddine and A. Peremans, Surf. Sci. **368**, 377 (1996).

[24] D. E. Gragson, B. M. McCarty, G. L. Richmond, and D. S. Alavi, J. Opt. Soc. Am. B **13**, 2075 (1996).

[25] X. Zhuang, D. Wilk, L. Marrucci, and Y. R. Shen, Phys. Rev. Lett. **75**, 2144 (1995).

[26] C. D. Stanners, Q. Du, R. P. Chin, P. Cremer, G. A. Somorjai, and Y. R. Shen, Chem. Phys. Lett. **232**, 407 (1995).

[27] G. R. Bell, C. D. Bain, and R. N. Ward, J. Chem. Soc., Faraday Trans. **92**, 515 (1996).

[28] R. N. Ward, D. C. Duffy, G. R. Bell, and C. D. Bain, Mol. Phys. **88**, 269 (1996).

[29] R. Braun, B. D. Casson, and C. D. Bain, Chem. Phys. Lett. **245**, 326 (1995).

[30] S. R. Hatch, R. S. Polizzotti, S. Dougal, and P. Rabinowitz, J. Vac. Sci. Technol. A **11**, 2232 (1993).

[31] H. Yamamoto, N. Akamatsu, A. Wada, K. Domen, and C. Hirose, J. Electron Spectrosc. Relat. Phenom. **64/65**, 507 (1993).

[32] D. Zhang, J. H. Gutow, T. F. Heinz, and K. B. Eisenthal, J. Phys. Chem. **98**, 13 729 (1994).

[33] K. Wolfrum and A. Laubereau, Chem. Phys. Lett. **228**, 83 (1994).

[34] D. A. Cadenhead, in *Structure and Properties of Cell Membranes*, edited by G. Benga (CRC, Boca Raton, FL, 1985), Vol. III, p. 22.

[35] G. Berkovic, Th. Rasing, and Y. R. Shen, J. Opt. Soc. Am. B **4**, 945 (1987).

[36] T. G. Zhang, C. H. Zhang, and G. K. Wong, J. Opt. Soc. Am. B **7**, 902 (1990).

[37] T. F. Heinz, H. W. K. Tom, and Y. R. Shen, Phys. Rev. A **28**, 1883 (1983).

[38] M. S. Johal, E. W. Usadi, and P. B. Davies, J. Chem. Soc., Faraday Trans. **92**, 573 (1996).

[39] H. Hsiung, G. R. Meredith, H. Vanherzeele, R. Popovitz-Biro, E. Shavit, and M. Lahav, Chem. Phys. Lett. **164**, 539 (1989).

[40] G. Cnossen, K. E. Drabe, and D. A. Wiersma, J. Phys. Chem. **97**, 4512 (1992).

[41] R. M. Corn and D. A. Higgins, in *Characterization of Organic Thin Films*, edited by A. Ulman (Butterworth-Heinemann, Boston, 1995), pp. 227–247.
[42] B. D. Casson and C. D. Bain, Langmuir **13**, 5465 (1997).
[43] In the case of SFG, the *first* two indices of $\chi^{(2)}$ are also interchangeable, if the sum-frequency and visible beams are away from electronic resonances.
[44] J. Y. Zhang, J. Y. Huang, Y. R. Shen, and C. Chen, J. Opt. Soc. Am. B **10**, 1758 (1993).
[45] R. A. MacPhail, H. L. Strauss, R. G. Snyder, and C. A. Elliger, J. Phys. Chem. **88**, 334 (1984).
[46] P. Guyot-Sionnest, J. H. Hunt, and Y. R. Shen, Phys. Rev. Lett. **59**, 1597 (1987).
[47] Several schemes for obtaining the orientation of $CH_3$ groups of an alkyl chain by SFG have been discussed in the literature. Bain and coworkers have critically reviewed them recently (Ref. 27).
[48] M. R. Querry, D. M. Wieliczka, and D. J. Segelstein, in *Handbook of Optical Constants of Solids II*, edited by E. D. Palik (Academic, Boston, 1991), pp. 1059–1077.
[49] J. Majewski, R. Popovitz-Biro, W. G. Bouwman, K. Kjaer, J. Als-Nielsen, M. Lahav, and L. Leiserowitz, Chem.-Eur. J. **1**, 304–311 (1995).
[50] *Refractive Indices of Pure Liquids and Binary Mixtures*, edited by M. D. Lechner, Landolt-Börnstein, New Series, Group III, Vol. 38, Pt. 6 (Springer, Berlin, 1996).
[51] F. Allen (private communication).
[52] S. Ramdas and J. M. Thomas, J. Chem. Soc., Faraday Trans. 2 **72**, 1251 (1976).
[53] T. Hanemann, W. Haase, I. Svoboda, and H. Fuess, Liq. Cryst. **19**, 699 (1995).
[54] G. Celebre, M. Longeri, E. Sicilia, and J. W. Emsley, Liq. Cryst. **7**, 731 (1990).
[55] J. D. Jackson, *Classical Electrodynamics*, 2nd ed. (Wiley, New York, 1975).